

Accepted Manuscript

Anomalous reversal of transverse thermoelectric voltage in $\text{CoFe}_{100-x}/\text{YIG}$ junction

R. Ramos, P. Wongjom, R. Iguchi, A. Yagmur, Z. Qiu, S. Pinitsoontorn, K. Uchida, E. Saitoh

PII: S0304-8853(17)31885-1

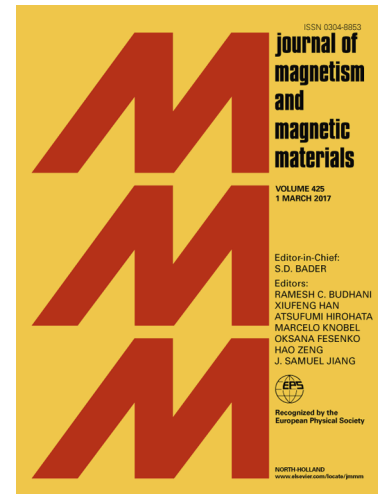
DOI: <http://dx.doi.org/10.1016/j.jmmm.2017.09.034>

Reference: MAGMA 63163

To appear in: *Journal of Magnetism and Magnetic Materials*

Please cite this article as: R. Ramos, P. Wongjom, R. Iguchi, A. Yagmur, Z. Qiu, S. Pinitsoontorn, K. Uchida, E. Saitoh, Anomalous reversal of transverse thermoelectric voltage in $\text{CoFe}_{100-x}/\text{YIG}$ junction, *Journal of Magnetism and Magnetic Materials* (2017), doi: <http://dx.doi.org/10.1016/j.jmmm.2017.09.034>

This is a PDF file of an unedited manuscript that has been accepted for publication. As a service to our customers we are providing this early version of the manuscript. The manuscript will undergo copyediting, typesetting, and review of the resulting proof before it is published in its final form. Please note that during the production process errors may be discovered which could affect the content, and all legal disclaimers that apply to the journal pertain.



Anomalous reversal of transverse thermoelectric voltage in $\text{Co}_\delta\text{Fe}_{100-\delta}/\text{YIG}$ junction

R. Ramos^{a,*}, P. Wongjom^b, R. Iguchi^{c,d}, A. Yagmur^{c,d}, Z. Qiu^a, S.
Pinitsoontorn^b, K. Uchida^{c,d,e,f}, E. Saitoh^{a,c,f,g}

^a*Advanced Institute for Materials Research, Tohoku University, Sendai 980-8577, Japan*

^b*Integrated Nanotechnology Research Center, Department of Physics, Faculty of Science,
Khon Kaen University, Khon Kaen, 40002, Thailand*

^c*Institute for Materials Research, Tohoku University, Sendai 980-8577, Japan*

^d*National Institute for Materials Science, Tsukuba 305-0047, Japan*

^e*PRESTO, Japan Science and Technology Agency, Saitama 332-0012, Japan*

^f*Center for Spintronics Research Network, Tohoku University, Sendai 980-8577, Japan*

^g*Advanced Science Research Center, Japan Atomic Energy Agency, Tokai 319-1195,
Japan*

Abstract

We have studied thermoelectric conversion in all-ferromagnetic $\text{Co}_\delta\text{Fe}_{100-\delta}/\text{YIG}$ bilayer junctions as a function of the chemical composition δ . We performed measurements of the transverse thermoelectric voltage upon application of a magnetic field. The voltage measured in the longitudinal spin Seebeck effect configuration shows a sign reversal at $\delta = 40\%$, which cannot be explained by the conventional electronic transport, such as the anomalous Nernst and Hall effects in the $\text{Co}_\delta\text{Fe}_{100-\delta}$ layer. Our results suggest a possible role of the sd-type exchange interaction between $\text{Co}_{40}\text{Fe}_{60}$ and YIG at the interface as a possible origin for the observed behavior.

Keywords: Spintronics, Spin caloritronics, Spin Seebeck effect, Anomalous Nernst effect

1. Introduction

The interaction between heat, spin and charge degrees of freedom is the central topic of the field of spin caloritronics [1, 2]. One of the most promi-

*Corresponding author

Email address: ramosr@imr.tohoku.ac.jp (R. Ramos)

ment effects studied within the field is the spin Seebeck effect (SSE) [3]: the spin counterpart of the conventional Seebeck effect. The SSE consists in the thermal generation of spin currents in a magnetic material. In contrast to conventional Seebeck effect, the SSE has also been observed in ferrimagnetic insulators (FI) [4, 5], expanding the range of available materials for SSE studies [6, 7, 8, 9, 10, 11, 12], and having the potential advantage of thermoelectric generation, due to the absence of mobile carriers in FI. Moreover, the SSE geometry is advantageous for the implementation of thin film and flexible thermoelectric devices [13, 14]. However, the magnitude of the extractable power is one of the main roadblocks for achieving a functional device [15, 16]. Extensive efforts are currently being devoted in this direction, such as spin Hall thermopiles, multilayer devices [17, 18, 19, 20, 21, 22] or bulk composites [23].

In the SSE, the thermally generated spin currents are detected by means of the inverse spin Hall effect (ISHE) in an adjacent paramagnetic metal (P) as an electric field given by the expression:

$$\mathbf{E}_{\text{ISHE}} = \theta_{\text{SH}}\rho(\mathbf{J}_S \times \sigma), \quad (1)$$

where θ_{SH} and ρ denote the spin Hall angle and electric resistivity of P, respectively. \mathbf{E}_{ISHE} , \mathbf{J}_S , and σ are the electric field, spatial direction of spin current (perpendicular to the P/FI interface) and spin-polarization vector (parallel to the magnetization, \mathbf{M}). Platinum is one of the most commonly used materials for ISHE detection, due to its comparatively large spin-Hall angle [24, 25], although the spin-charge conversion efficiency is about 10% and it is also a non cost-effective material.

Recently, the ISHE in ferromagnetic metals (FM) has been reported [26, 27, 28, 29], with the observation of a relatively large spin Hall angle for permalloy (Py) [26, 27]. In FM materials the transverse thermoelectric voltage results from the combined effect of the SSE and anomalous Nernst effect (ANE), since both share the same experimental geometry [see Fig. 1(a)]. The ANE generated electric field can be expressed as:

$$\mathbf{E}_{\text{ANE}} = Q_S\mu_0(\nabla T \times \mathbf{M}) \quad (2)$$

where μ_0 and Q_S are the vacuum permeability and ANE coefficient, respectively. The observation of the ISHE in other antiferromagnets [30, 31, 32] and ferromagnets [26, 27, 28, 33, 34, 35], has opened the possibility to explore a wider range of materials, which are fundamentally interesting, due

to the possibility to study the interrelation between the ISHE and conventional magnetotransport properties. Furthermore, this type of systems are potentially advantageous for applications, since they can lead to increased thermoelectric conversion efficiencies due to hybrid voltage generation by means of additive contributions from the SSE and ANE in the FM layer. Here, we performed a systematic study of the transverse thermoelectric effect in $\text{Co}_\delta\text{Fe}_{100-\delta}/\text{YIG}$ system and compare it to its conventional thermoelectric and electric transport properties. It has been previously shown that the sign of the spin Hall angle in the transition metals can be tuned by the d -orbital filling [34, 36, 37], therefore by studying the $\text{Co}_\delta\text{Fe}_{100-\delta}$ electrode system we may get further information about the effect of orbital filling on the ISHE in the ferromagnetically ordered $3d$ transition metal system.

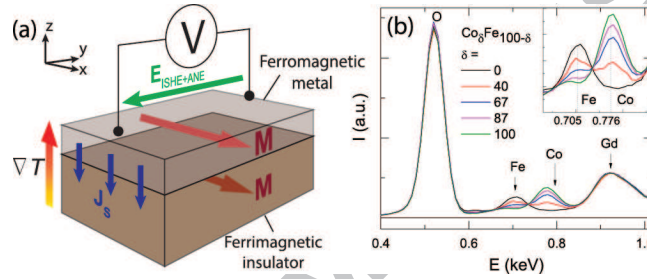


Figure 1: (a) A schematic illustration of hybrid thermoelectric generation by combined SSE and ANE in a bilayer system formed by the junction of a ferromagnetic metal (FM) and a ferrimagnetic insulator (FI) using the longitudinal spin Seebeck effect measurement geometry. (b) An EDX spectrum of the $\text{Co}_\delta\text{Fe}_{100-\delta}/\text{GGG}$ for δ ranging from 0 (Fe) to 100% (Co). Inset shows detail of Fe and Co L_α peaks.

2. Material and methods

The $\text{Co}_\delta\text{Fe}_{100-\delta}$ (10 nm) FM electrodes of different compositions were deposited, by electron beam evaporation, on isostructural paramagnetic insulator $\text{Gd}_3\text{Ga}_5\text{O}_{12}(111)$ (GGG) and ferrimagnetic insulator $\text{YIG}(112\ \mu\text{m})(111)/\text{GGG}(111)$ single crystalline substrates, also referred to as PI and FI, respectively. The GGG substrate thickness is $L_z = 0.4$ mm. The YIG film was grown by a liquid phase epitaxy method; its exact composition is $\text{Bi}_{0.04}\text{Y}_{2.96}\text{Fe}_5\text{O}_{12}$. Bi is used to improve the lattice matching between YIG and GGG. Therefore structural induced effects, due to the different substrates, on the magnetic

properties of $\text{Co}_\delta\text{Fe}_{100-\delta}$ films are expected to be negligible. Prior to the deposition of the FM electrodes the substrates were polished with alumina slurry. The $\text{Co}_\delta\text{Fe}_{100-\delta}$ films with nominal compositions $\delta = 100, 90, 75, 50$ and 0% were grown by electron-beam evaporation at room temperature. Two type of structures were simultaneously deposited for each composition on both substrates: a film covering the entire substrate with dimensions of $L_x = 2\text{ mm}$, $L_y = 6\text{ mm}$ for thermoelectric measurements, and Hall bar structures for resistivity and anomalous Hall effect (AHE) measurements. All the measurements were performed at room temperature.

The composition of the FM electrodes was evaluated using electron-dispersive X-ray analysis (EDX), measured on the films deposited on GGG substrates to avoid Fe contribution from YIG. The measured spectra is shown in Fig. 1(b), where the composition of the electrodes was evaluated by analysing the height of the Fe and Co peaks for each film. The values of δ were then estimated by linear extrapolation, assuming that the Fe (Co) peak height for Fe (Co) film corresponds to $\delta = 0\%$ (100%). We obtained the following estimated (nominal) values of δ in percentage: 100 (100), 87 (90), 67 (75), 40 (50) and 0 (0) %. The transport measurements were performed in a physical property measurement system (Quantum design, PPMS DynaCool) with a maximum magnetic field (H) of 90 kOe. For the thermoelectric measurements, the sample is placed between two AlN plates with large thermal conductivity. The thermal gradient is generated by passing a current to a resistive heater attached to the top plate, and the lower plate works as the heat sink. In order to minimize variations in thermal resistance between sample and AlN plate [38, 39], the thermal contact was kept homogeneous for all the measurements on different samples. The temperature difference (ΔT) between the plates is monitored by two thermocouples connected differentially. We performed measurements of the transverse thermoelectric voltage ($\parallel y$) by applying a thermal gradient across the FM/FI interface ($\parallel z$), while H is swept in the in-plane ($\parallel x$) direction. This configuration, so-called in-plane magnetized (IM) configuration [40], is conventionally used for the detection of the longitudinal SSE.

3. Results and discussion

First, we performed measurements of the transverse voltage in the IM configuration for the $\text{Co}_\delta\text{Fe}_{100-\delta}$ /YIG system as a function of the ferromag-

netic electrode composition (δ). The results are shown in Fig. 2(a)-(e): as the composition of the FM electrode is varied from Co ($\delta = 100\%$) to Fe ($\delta = 0\%$), the voltage magnitude gradually changes, and a sign reversal of the voltage is observed for $\delta = 40$ and 0% . Similar measurements were performed for $\text{Co}_\delta\text{Fe}_{100-\delta}$ electrodes grown on GGG, here the sign reversal of the voltage is only observed for the Fe electrode. This result suggests that the sign reversal observed in $\text{Co}_{40}\text{Fe}_{60}/\text{YIG}$ is due not to the compositional dependence of the ANE, possibly pointing to a compositional dependence of the ISHE and/or an important role of the FM/FI interface. Moreover, the magnetic field dependence of the transverse voltage for $\text{Co}_x\text{Fe}_{100-x}$ grown on YIG and GGG substrates show clear differences; with the voltage in GGG substrate saturating at low fields, while for YIG substrates the samples exhibit a strong magnetic field dependence over a wide field range, which cannot be explained by the normal Nernst effect of the FM. Another possibility could be due to a contribution from the paramagnetic SSE of GGG to the measured voltage, however the paramagnetic SSE in GGG has only been observed at low temperatures [41]. Moreover, the voltage in the $\text{Co}_\delta\text{Fe}_{100-\delta}/\text{GGG}$ samples show no high magnetic field dependence, suggesting that the paramagnetic SSE does not play a role in our measurements. It could be argued that the observed dependence can be due to the appearance of an out-of-plane anisotropy, as it was shown in ultrathin CoFe films [42], and/or a possible role of the exchange interaction across the interface in the observed voltage response.

In order to further explore the origin of the observed sign reversal, we measured the ANE in the perpendicular magnetized (PM) configuration [see inset of Fig. 2(f)], where H is applied parallel to z while the thermal gradient is stabilised in the in-plane ($\parallel x$) direction and the transverse voltage ($\parallel y$) is measured. In this configuration the ANE can still be observed, however the SSE is forbidden due to the ISHE geometry ($\mathbf{J}_s \parallel \mathbf{M}$) [27, 43]. This measurement allows us to clarify whether or not the observed behavior in $\text{Co}_{40}\text{Fe}_{60}/\text{YIG}$ is due to the ANE. Moreover, using the PM configuration we can also investigate whether the observed high magnetic field dependence is due to the change in magnetic anisotropy of the FM electrodes, since if perpendicular induced anisotropy is present in the $\text{Co}_\delta\text{Fe}_{100-\delta}/\text{YIG}$ system, the films should be easier to saturate with H applied in the out-of-plane direction ($\parallel z$). Figures 2(f)-(j) show the obtained results: no sign reversal appears in $\text{Co}_{40}\text{Fe}_{60}$ films grown on either GGG or YIG templates, with the sign reversal only present for the Fe films. Furthermore, there are no signif-

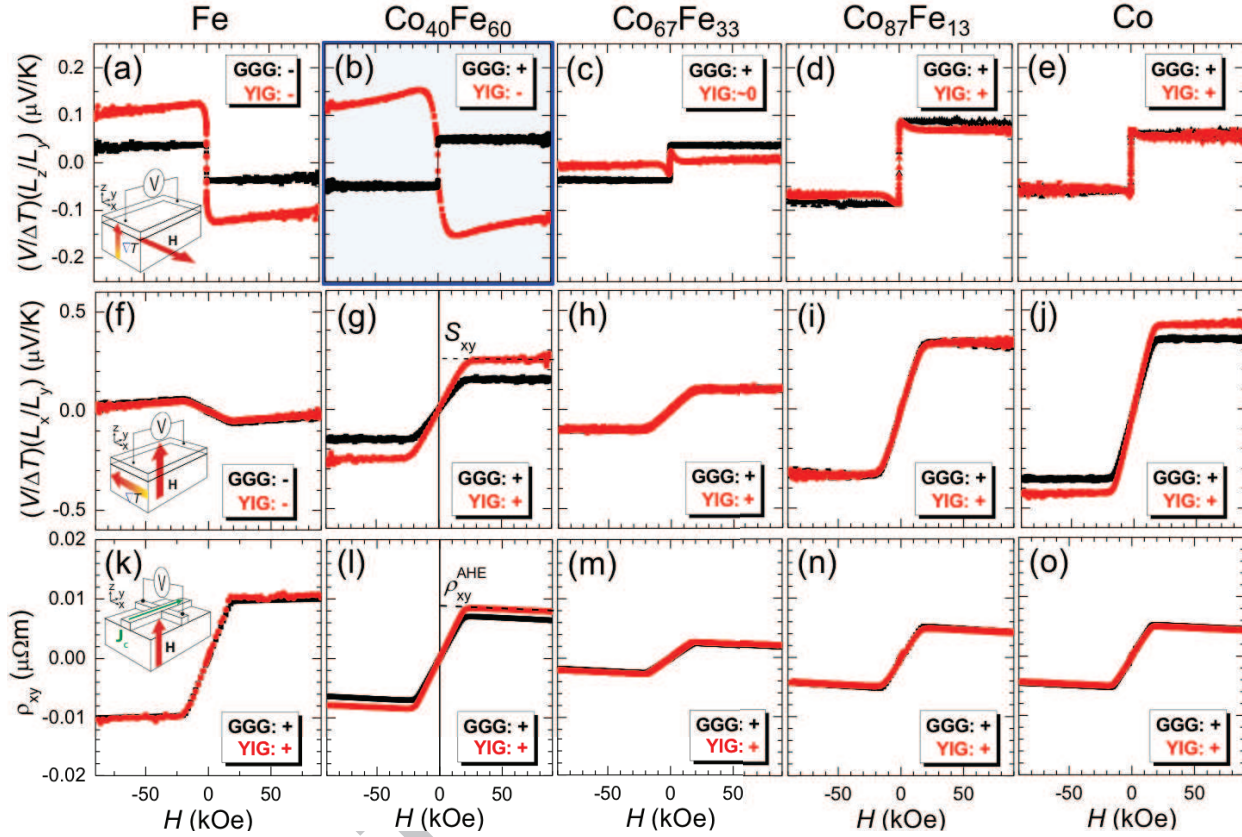


Figure 2: Thermal and electric magnetotransport properties of the $\text{Co}_\delta\text{Fe}_{1-\delta}/\text{GGG}$ and $\text{Co}_\delta\text{Fe}_{1-\delta}/\text{YIG}$ systems as a function of composition δ . (a-e) Transverse thermoelectric voltage measured with an in-plane magnetic field (longitudinal SSE configuration) and (f-j) with a magnetic field applied in the direction parallel to the surface normal (perpendicular magnetized configuration). (k-o) measured anomalous Hall effect (AHE).

icant differences in the magnetic field dependence between the FM/FI and FM/PI system, with the voltage saturating at similar magnetic fields for all compositions (δ), independent of the substrates employed. These measurements confirm that the observed sign reversal in the $\text{Co}_{40}\text{Fe}_{60}/\text{YIG}$ system cannot be explained by the conventional ANE and that there is no significant perpendicular magnetic anisotropy present in the system, and therefore other mechanism must be responsible for the sign reversal of the transverse voltage in $\text{Co}_{40}\text{Fe}_{60}/\text{YIG}$.

Other possibility could be the compositional dependence of the ISHE in $\text{Co}_\delta\text{Fe}_{100-\delta}$ system, as it has been previously shown for $3d$ transition metals [34], where the ISHE presents a sign reversal upon increasing the number of the d electrons in the system. Since the ISHE and anomalous Hall effect (AHE) share the same origin (they both depend on the spin-orbit interaction) [24, 25, 44], we performed AHE measurements in $\text{Co}_\delta\text{Fe}_{100-\delta}/\text{YIG}$ and $\text{Co}_\delta\text{Fe}_{100-\delta}/\text{GGG}$. The results are shown in Fig. 2(k)-(o), we can see that the sign of the AHE voltage remains unaffected for the different FM compositions. The AHE shows a reduction in magnitude for $\delta = 67\%$, consistent with the reported low magnetotransport coefficients for this composition [45]. The voltage at high magnetic fields presents a negative slope for all compositions, except for Fe in which a positive slope is observed; this is in agreement with the previous reports of the AHE in Fe and Co thin films [46, 47].

In order to further evaluate the thermoelectric transport properties of the $\text{Co}_\delta\text{Fe}_{100-\delta}$ system, we also measured the compositional dependence of the conventional Seebeck effect for the $\text{Co}_\delta\text{Fe}_{100-\delta}$ electrodes [see Fig. 3(a)], the results are similar to the ANE results, where a sign reversal is present only for Fe, in agreement with the change of polarity in the high field slope observed in the Hall effect measurements.

Now we are in a position to analyse the data considering the expression $J_i = \sigma_{ij}E_j - \alpha_{ik}\nabla_k T$, where J_i stands for the electron current, E_j is the electric field, $\nabla_k T$ is the applied thermal gradient, and the coefficients σ_{ij} and α_{ik} are the elements of the electrical and thermoelectric conductivity tensors, respectively. Under the open circuit condition ($J_y = 0$), the following expression of the ANE electric field is obtained:

$$E_y = [\rho\alpha_{xy} - S\tan\theta_{xy}]\nabla_x T, \quad (3)$$

where ρ is the thin film resistivity, $S = \rho\alpha_{xx}$ is the Seebeck coefficient and $\tan\theta_{xy} = \rho_{xy}/\rho$ is the Hall angle, where we consider the Hall angle estimated from the AHE transverse resistivity, ρ_{xy}^{AHE} [see Fig. 2(1)]. The first term of

the equation arises from the non-diagonal component of the thermoelectric conductivity tensor and the second term is given by the combined contribution of the Seebeck and AHE effects.

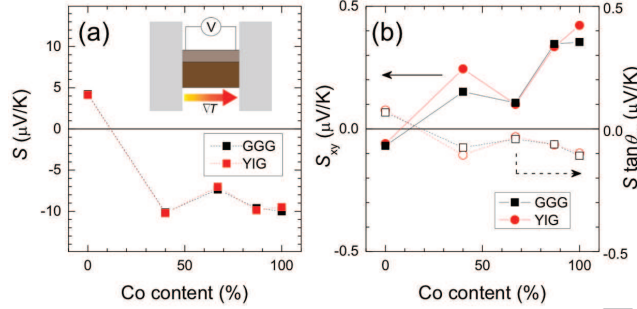


Figure 3: (a) Conventional Seebeck coefficient as a function of electrode composition measured at room temperature on GGG and YIG. (b) Left axis (solid symbols) shows the measured anomalous Nernst coefficients obtained from the perpendicular magnetized measurement for different composition of ferromagnetic electrodes. Right axis (empty symbols) shows the contribution from the combined effect of Seebeck and anomalous Hall effect.

Figure 3(b) summarises the conventional thermoelectric coefficients for the $\text{Co}_\delta\text{Fe}_{100-\delta}$ system, representing the ANE coefficient measured in the PM configuration, S_{xy} [see Fig. 2(g)] and the second term of Eq. 3, proportional to the combined contribution from Seebeck and AHE effects ($S \tan \theta_{xy}$). We can clearly see that the sign reversal observed in $\text{Co}_{40}\text{Fe}_{60}/\text{YIG}$ in the in-plane magnetized (longitudinal SSE) configuration cannot be explained by the conventional thermoelectric transport properties, where the sign reversal is only present in Fe. Moreover, the AHE data shown previously suggests that the observed sign reversal cannot be explained by the compositional dependence of the AHE, suggesting that the bulk spin-orbit properties of the $\text{Co}_\delta\text{Fe}_{100-\delta}$ system are not responsible for the sign reversal of the transverse thermoelectric voltage, and possibly pointing to the role of the FM/FI interface in the observed behavior [48].

To confirm the importance of the interfacial exchange interaction at the FM/FI interface, we performed measurements for a sample where a Cu layer of 5 nm was inserted between the $\text{Co}_{40}\text{Fe}_{60}$ film and the YIG substrate. Figure 4 shows the transverse thermoelectric response measured in the IM configuration compared to that previously observed with no Cu insertion layer. It can be clearly seen that the sign reversal and the high magnetic

field dependence of the voltage disappear. This suggests again that the direct contact between YIG and $\text{Co}_{40}\text{Fe}_{60}$ is essential for the observation of the sign reversal.

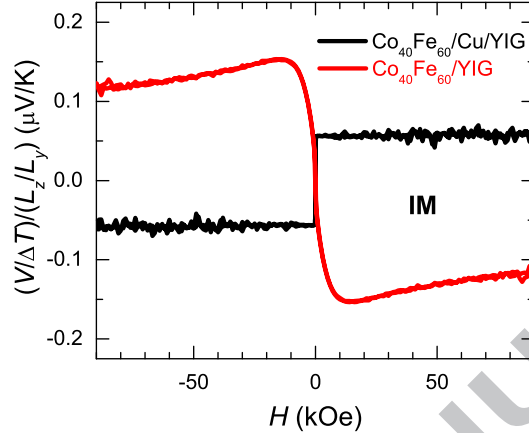


Figure 4: Effect of a Cu insertion layer on the transverse thermoelectric response of $\text{Co}_{40}\text{Fe}_{60}$ measured in the in-plane magnetized configuration.

Let us now discuss one possible scenario for the observed results. Here, we will consider a propagating spin current at the FM/FI interface. When a thermal gradient is applied parallel to the z direction, due to the spin-dependent Seebeck effect of the FM, a spin accumulation can be induced at the FM/FI interface [49]. Here, due to the continuity of the spin current, the spin accumulation of the FM can decay by spin-flip scattering of conduction electrons at the interface, through the sd-type exchange interaction [50] with local moments of the FI, allowing for the spin current to propagate through the FM/FI interface [51, 52]. This process induces a non-equilibrium shift of the spin-dependent chemical potentials (and the interface spin-polarization), which can possibly affect the spin-dependent electronic properties of the FM at the interface, resulting in an interface-induced ANE. Indeed, previous theoretical studies have shown that the ANE in the 3d ferromagnetic metals is highly sensitive to the position of the Fermi level (and therefore the spin polarization) [53]. The electronic structure of $\text{Co}_{\delta}\text{Fe}_{100-\delta}$ is strongly dependent on the composition δ : Fe has both up- and down-spin bands crossing the Fermi level (E_F) and, as the Co content increases, the additional electrons populate the majority spin states, which shifts down the band and it becomes

filled at an intermediate value of about $\delta = 30\%$ [54, 55]. Since $\text{Co}_{40}\text{Fe}_{60}$ is very close to the δ value where the majority spin band becomes totally filled. The above described process might have stronger implications in the spin-dependent transport properties for this composition, which might be a possible reason behind the observed differences between $\text{Co}_{40}\text{Fe}_{60}/\text{YIG}$ and $\text{Co}_{40}\text{Fe}_{60}/\text{GGG}$. However, the magnetic field dependence in $\text{Co}_{\delta}\text{Fe}_{100-\delta}/\text{YIG}$ cannot be interpreted even under this scenario, implying the coexistence of other mechanisms, such as a possible contribution from the magnon spin currents of the $\text{Co}_{\delta}\text{Fe}_{100-\delta}$ layer.

4. Conclusion

In summary, we measured spin dependent thermoelectric properties of $\text{Co}_{\delta}\text{Fe}_{100-\delta}$ alloy in a fully ferromagnetic FM/FI system. We have observed an unexpected sign reversal of the transverse thermoelectric voltage for an alloy composition of $\delta = 40\%$, which cannot be explained by the conventional transport properties. Our results possibly suggest the presence of an interface-driven ANE, where the role of the sd-type exchange at the $\text{Co}_{40}\text{Fe}_{60}/\text{YIG}$ layer might be important to understand the observed behavior. These results also show the possibility of tuning the polarity of the spin-induced thermoelectric response, which can be beneficial for fabrication of thermoelectric devices based on all-ferromagnetic system, such as spin Seebeck thermopiles.

5. Acknowledgments

The authors thank J. Barker and G. E. W. Bauer for valuable discussions. This work was supported by JST ERATO Grant Number JPMJER1402, and PRESTO "Phase Interfaces for Highly Efficient Energy Utilization" (JPMJPR12C1) from JST, Japan, Grant-in-Aid for Scientific Research on Innovative Areas "Nano Spin Conversion Science" (26103005), Grant-in-Aid for Scientific Research (A) (15H02012) from MEXT, Japan, NEC Corporation, and The Noguchi Institute.

- [1] G. E. W. Bauer, E. Saitoh, and B. J. van Wees, *Nat. Mater.* **11**, 391 (2012).

- [2] S. R. Boona, R. C. Myers, and J. P. Heremans, *Energy Environ. Sci.* **7**, 885 (2014).
- [3] K. Uchida, S. Takahashi, K. Harii, J. Ieda, W. Koshibae, K. Ando, S. Maekawa, and E. Saitoh, *Nature* **455**, 778 (2008).
- [4] K. Uchida, J. Xiao, H. Adachi, J. Ohe, S. Takahashi, J. Ieda, T. Ota, Y. Kajiwara, H. Umezawa, H. Kawai, et al., *Nat. Mater.* **9**, 894 (2010).
- [5] K. Uchida, H. Adachi, T. Ota, H. Nakayama, S. Maekawa, and E. Saitoh, *Appl. Phys. Lett.* **97**, 172505 (2010).
- [6] R. Ramos, T. Kikkawa, K. Uchida, H. Adachi, I. Lucas, M. H. Aguirre, P. Algarabel, L. Morellón, S. Maekawa, E. Saitoh, et al., *Appl. Phys. Lett.* **102**, 072413 (2013).
- [7] D. Meier, T. Kuschel, L. Shen, A. Gupta, T. Kikkawa, K. Uchida, E. Saitoh, J.-M. Schmalhorst, and G. Reiss, *Phys. Rev. B* **87**, 054421 (2013).
- [8] T. Niizeki, T. Kikkawa, K. Uchida, M. Oka, K. Z. Suzuki, H. Yanagihara, E. Kita, and E. Saitoh, *AIP Advances* **5**, 053603 (2015).
- [9] K. Uchida, T. Kikkawa, A. Miura, J. Shiomi, and E. Saitoh, *Phys. Rev. X* **4**, 041023 (2014).
- [10] E.-J. Guo, A. Herklotz, A. Kehlberger, J. Cramer, G. Jakob, and M. Kläui, *Appl. Phys. Lett.* **108**, 022403 (2016).
- [11] A. Anadón, R. Ramos, I. Lucas, P. A. Algarabel, L. Morellón, M. R. Ibarra, and M. H. Aguirre, *Appl. Phys. Lett.* **109**, 12404 (2016).
- [12] P. Jiménez-Cavero, I. Lucas, A. Anadón, R. Ramos, T. Niizeki, M. H. Aguirre, P. A. Algarabel, K. Uchida, M. R. Ibarra, E. Saitoh, et al., *APL Materials* **5**, 026103 (2017).
- [13] A. Kirihara, K. Uchida, Y. Kajiwara, M. Ishida, Y. Nakamura, T. Manako, E. Saitoh, and S. Yoroazu, *Nat. Mater.* **11**, 686 (2012).
- [14] A. Kirihara, K. Kondo, M. Ishida, K. Ihara, Y. Iwasaki, A. Matsuba, K. Uchida, E. Saitoh, N. Yamamoto, and T. Murakami, *Sci. Rep.* **6**, 23114 (2016).

- [15] K. Uchida, M. Ishida, T. Kikkawa, a. Kirihara, T. Murakami, and E. Saitoh, *J. Phys.: Condens. Matter* **26**, 343202 (2014).
- [16] K. Uchida, H. Adachi, T. Kikkawa, A. Kirihara, M. Ishida, S. Yorozu, S. Maekawa, and E. Saitoh, *Proc. IEEE* **104**, 1946 (2016), 1604.00477.
- [17] K. Uchida, T. Nonaka, T. Yoshino, T. Kikkawa, D. Kikuchi, and E. Saitoh, *Appl. Phys. Express* **5**, 093001 (2012).
- [18] R. Ramos, T. Kikkawa, M. H. Aguirre, I. Lucas, A. Anad, T. Oyake, K. Uchida, and H. Adachi, *Phys. Rev. B* **92**, 220407(R) (2015).
- [19] R. Ramos, A. Anadon, I. Lucas, K. Uchida, P. A. Algarabel, L. Morellon, M. H. Aguirre, E. Saitoh, and M. R. Ibarra, *APL Mater.* **4**, 104802 (2016).
- [20] K. Uchida, T. Kikkawa, T. Seki, T. Oyake, J. Shiomi, Z. Qiu, K. Takanashi, and E. Saitoh, *Phys. Rev. B* **92**, 094414 (2015).
- [21] Y. Shiomi, Y. Handa, T. Kikkawa, and E. Saitoh, *Appl. Phys. Lett.* **106**, 232403 (2015).
- [22] K.-D. Lee, D.-J. Kim, H. Yeon Lee, S.-H. Kim, J.-H. Lee, K.-M. Lee, J.-R. Jeong, K.-S. Lee, H.-S. Song, J.-W. Sohn, et al., *Sci. Rep.* **5**, 10249 (2015).
- [23] S. R. Boona, K. Vandaele, I. N. Boona, D. W. McComb, and J. P. Heremans, *Nat Commun* **7**, 13714 (2016).
- [24] A. Hoffmann, *IEEE Trans. Magn.* **49**, 5172 (2013).
- [25] J. Sinoya, S. O. Valenzuela, J. Wunderlich, C. H. Back, and T. Jungwirth, *Rev. Mod. Phys.* **87**, 1213 (2015), 1411.3249.
- [26] B. F. Miao, S. Y. Huang, D. Qu, and C. L. Chien, *Phys. Rev. Lett.* **111**, 066602 (2013).
- [27] T. Kikkawa, K. Uchida, S. Daimon, Y. Shiomi, H. Adachi, Z. Qiu, D. Hou, X.-F. Jin, S. Maekawa, and E. Saitoh, *Phys. Rev. B* **88**, 214403 (2013).

- [28] D. Tian, Y. Li, D. Qu, X. Jin, and C. L. Chien, *Appl. Phys. Lett.* **106**, 212407 (2015).
- [29] D. Tian, Y. Li, D. Qu, S. Y. Huang, X. Jin, and C. L. Chien, *Phys. Rev. B* **94**, 020403(R) (2016).
- [30] L. Frangou, S. Oyarzún, S. Auffret, L. Vila, S. Gambarelli, and V. Baltz, *Phys. Rev. Lett.* **116**, 077203 (2016).
- [31] W. Zhang, M. B. Jungfleisch, W. Jiang, J. E. Pearson, and A. Hoffmann, *Phys. Rev. Lett.* **113**, 196602 (2014).
- [32] D. Qu, S. Y. Huang, and C. L. Chien, *Phys. Rev. B* **92**, 020418 (2015).
- [33] S. M. Wu, J. Hoffman, J. E. Pearson, and A. Bhattacharya, *Appl. Phys. Lett.* **105**, 092409 (2014).
- [34] C. Du, H. Wang, F. Yang, and P. C. Hammel, *Phys. Rev. B* **90**, 140407 (2014).
- [35] T. Seki, K. Uchida, T. Kikkawa, Z. Qiu, and E. Saitoh, *Appl. Phys. Lett.* **107**, 092401 (2015).
- [36] H. L. Wang, C. H. Du, Y. Pu, R. Adur, P. C. Hammel, and F. Y. Yang, *Phys. Rev. Lett* **112**, 197201 (2014).
- [37] C. Du, H. Wang, P. C. Hammel, F. Yang, C. Du, H. Wang, P. C. Hammel, and F. Yang, *J. Appl. Phys.* **117**, 172603 (2016).
- [38] A. Sola, M. Kuepferling, V. Basso, M. Pasquale, T. Kikkawa, K. Uchida, and E. Saitoh, *J. Appl. Phys.* **117**, 17C510 (2015).
- [39] A. Sola, P. Bougiatioti, M. Kuepferling, D. Meier, G. Reiss, M. Pasquale, T. Kuschel, and V. Basso, *Sci. Rep.* **7**, 46752 (2017).
- [40] T. Kikkawa, K. Uchida, Y. Shiomi, Z. Qiu, D. Hou, D. Tian, H. Nakayama, X.-F. Jin, and E. Saitoh, *Phys. Rev. Lett.* **110**, 067207 (2013).
- [41] S. M. Wu, J. E. Pearson, and A. Bhattacharya, *Phys. Rev. Lett.* **114**, 186602 (2015).

- [42] A. Sung-Min and G. S. D. Beach, *J. of Appl. Phys.* **113**, 17C112 (2013).
- [43] P. Bougiatioti, C. Klewe, D. Meier, O. Manos, O. Kuschel, J. Wollschläger, L. Bouchenoire, S. D. Brown, J.-M. Schmalhorst, G. Reiss, et al., arXiv:1702.05384 (2017).
- [44] S. Maekawa, H. Adachi, K. Uchida, J. Ieda, and E. Saitoh, *J. Phys. Soc. Jpn.* **82**, 102002 (2013).
- [45] S. M. Haidar, R. Iguchi, A. Yagmur, J. Lustikova, Y. Shiomi, and E. Saitoh, *J. Appl. Phys.* **117**, 183906 (2015).
- [46] M. Rubinstein, F. J. Rachford, W. W. Fuller, and G. A. Prinz, *Phys. Rev. B* **37**, 8689 (1988).
- [47] D. Hou, Y. Li, D. Wei, D. Tian, L. Wu, and X. Jin, *J. Phys.: Condens. Matter* **24**, 482001 (2012).
- [48] L. Zhou, V. L. Grigoryan, S. Maekawa, X. Wang, and J. Xiao, *Phys. Rev. B* **91**, 045407 (2015).
- [49] A. Slachter, F. L. Bakker, J.-P. Adam, and B. J. van Wees, *Nat. Phys.* **6**, 879 (2010).
- [50] S. Zhang and Z. Li, *Phys. Rev. Lett.* **93**, 127204 (2004).
- [51] S. Takahashi, E. Saitoh, and S. Maekawa, *Journal of Physics: Conference Series* **200**, 62030 (2010).
- [52] S. S.-L. S. Zhang and S. S.-L. S. Zhang, *Phys. Rev. B* **86**, 214424 (2012).
- [53] J. Weischenberg, F. Freimuth, S. Blügel, and Y. Mokrousov, *Phys. Rev. B* **87**, 060406(R) (2013).
- [54] R. Richter and H. Eschrig, *J. Phys. F: Met. Phys.* **18**, 1813 (1988).
- [55] M. Ležaić, P. Mavropoulos, and S. Blügel, *Appl. Phys. Lett.* **90**, 082504 (2007), 0612497.

Highlights

- The thermoelectric conversion is systematically investigated in $\text{Co}_\delta\text{Fe}_{100-\delta}$ /YIG bilayer junctions as a function of the chemical composition δ .
- The voltage measured in the longitudinal spin Seebeck effect configuration shows a sign reversal at $\delta = 40\%$
- The reversal cannot be understood by conventional electronic transport properties of $\text{Co}_\delta\text{Fe}_{100-\delta}$.
- The results suggest the presence of an interface-driven ANE.
- These results show the possibility of tuning the polarity of the spin-induced thermoelectric response